SciMedCentral

JSM Chemistry

Original Article

Electrochemical Determination of Nicotine in Cigarette, and Urine Using *para*-Aminobenzene Sulfonic Acid Grafted Screen Printed Carbon Electrode

Tesfu Hailu[1,3]*, Yaw-Kuen Li[2], and Merid Tessema[1,2]

[1]*Department of industrial chemistry, Addis Ababa Science and Technology University, Addis Ababa P.O.Box 16417, Ethiopia.*

[2]*Department of applied chemistry, 1001 University Road, Hsinchu, Taiwan 300, ROC*

[3]*Department of chemistry, Addis Ababa University College of Natural and Computational Science, Addis Ababa P.O.Box 1176*

***Corresponding author**

Tesfu Hail, Department of industrial chemistry, Addis Ababa Science and Technology University, Addis Ababa P.O.Box 16417, Ethiopia. Email: tesfuyee@gmail.com

Submitted: 18 May 2021

Accepted: 24 June 2021

Published: 26 June 2021

ISSN: 2333-6633

Keywords

- Activated
- Grafting
- Nicotine
- *para*-Aminobenzene sulfonic acid and screen printed carbon electrode

Abstract

In this study, a simple, scalable, and low-cost electrochemically grafted screen printed carbon electrode was developed for sensitive and selective determination of nicotine. First, simple and fast activation of bare screen printed carbon electrode was performed by linear sweep voltammetry using KOH solution, then the electrode is grafted electrochemically using in-situ generated *para*-aminobenzene sulfonic acid diazonium salt and was used for the determination of nicotine. The voltammetric study of nicotine in Britton Robinson buffer solution pH 8.0 showed an electrocatalytic effect towards nicotine oxidation, which cause in a larger current response when matched with the bare. Under the optimized conditions, a linear calibration curve was obtained using square wave voltammetry at the *para*-aminobenzene sulfonic acid grafted electrode in the range of 0.5-300 μM with detection and quantification limit 0.35 μM and 1.14 μM, respectively.

INTRODUCTION

Nicotine, is an alkaloid abundantly found in the nightshade family of plants called Nicotiana tabacum L., Solanaceae, and is the main component of tobacco [1]. High-dose nicotine intake causes bradycardia, hypotension, and depressed mental status due to ganglionic blockade [2]. However, there are finding on the harmfulness of orally ingested nicotine; possibly lethal doses of it can be ingested by excessive use of electronic cigarettes [1]. On the contrary, research findings showed that nicotine has therapeutic use particularly in cardiovascular, respiratory disorders in lung cancer and age-related diseases like Alzheimer and Parkinson diseases [3]. Though, significant prove demonstrate the negative effect of tobacco towards COVID-19 including predisposition to the virus infection, the severity of progression, and mortality. There is report from examination of data from a number of independent studies that concludes that smoking is not associated with the severity of coronavirus disease although this assertion has been questioned. Up to present, some of the finding asserts there is smaller frequency in hospitalization of patient with COVID-19 from tobacco user [4].

Therefore, analysis of the sample for nicotine is crucial in the cigarette making plant as well as in forensic toxicology [5]. Over the past two decades, several analytical techniques including high-performance liquid chromatography [6-8], gas chromatography-mass spectrometry [9-11], high-performance capillary electrophoresis [12], capillary electrophoresis [13] capillary electrophoresis coupled with electrochemiluminescence [14] spectrophotometry [15, 16] were used for the determination of nicotine. But these methods are quite expensive require advanced technology knowledge with skill man power. Additionally, those techniques have critical disadvantage for there is a waste of the analyte while preparing, extracting, purifying it. The electrochemical techniques we used are favorable for the reason that they are economical, simple, easy and rapid [17]. Oxidation of a given analyte at higher potential is a common problem to detect it electrochemically, and nicotine is among these which oxidize at higher potential. Hence, an electrode that can effectively decrease the over-potential with an improved current is required for its determination. In this work, this is achieved by using *para*-aminobenzene sulfonic acid (*p*-ABSA) grafted screen printed carbon electrode (SPCE).

Grafting of diazonium salts electrochemically provides highly reactive aryl radicals that bind strongly to substrate surfaces through covalent bonding [18]. This covalent attachment to the carbon surfaces was performed by the oxidation of primary amines and the aryl diazonium cations reduction, which allows the attachment of organic moieties on carbon surfaces through C-C and N-C bonds [19].

EXPERIMENTAL

Materials and method

Nicotine, *p*-ABSA, sodium nitrite, hydrochloric acid, glucose, boric acid, acetic acid, phosphoric acid and uric acid were acquired from Sigma Aldrich and the SPCE was purchased from Zensor R&D Co., LTD, Taiwan. All the chemicals were used as it is without any treatment and the Nicotine solution was prepared using deionized water. Britton Robinson buffer in solution was used for nicotine determination.

Electrochemical tests were performed using CHI760D electrochemical workstation (CH Instruments, USA). The surface imaging of the electrodes was analyzed by JEOL JSM-7401F Field Emission *Scanning Electron Microscope. All the experiment was performed by drop coating SPCE that cover the* working electrode, Ag/AgCl pellet reference electrode, and carbon auxiliary electrode. The determination of NIV was studied using SWV in the potential range of 0.4 to 1.4 V with the optimized pulse amplitude (60 mV), step potential (10 mV), and frequency (40 Hz).

Grafting of SPCE

The electrode surface was modified by grafting electrochemically using an in-situ generated *p*-ABSA diazonium ion as described [20]. In brief, the diazonium cation was synthesized by an in-situ reaction in which $NaNO_2$ solution was dropped to an ice-cold 5 mM *p*-ABSA solution in 0.5 M HCl to form its final concentration 10 mM. Then the mixture was left to react for 5 minutes in an ice bath. Finally, the grafting of the SPCE was done by drop-casting the cold solution and cycling by linear sweep voltammetry from 0.0 to −1.0 V for 15 cycles at 100 mV s^{-1}. After modification, the electrode was cleaned by running distilled water, flushed with nitrogen, and was utilized without any advanced treatment.

Preparation of Urine Sample

A human urine sample was collected from a wholesome volunteer and kept in sterilized plastic containers. Initially, using a magnetic stirrer, the urine become stirred for 5 minutes and filtered using Whatman filter paper to attain a transparent filtrate. Then, from the filtrate 5 mL was taken and spilled right into a 50 mL volumetric flask and using a BRB solution of pH 8.0 the flask was crammed to the mark. To investigate the recovery analysis, different concentrations of nicotine standards were added to the filtrate, which was then analyzed using SWV.

Extraction of Nicotine from Cigarette

Cigarette samples for analysis have been set in line with the procedure reported [21] and described as follows. First, the tobacco sample was collected in a clean watch glass by peeling the rolling paper. Then the tobacco sample was dried for two hours at 40 °C in a vacuum oven. Nicotine extraction was employed using ultra-sonication of the dry tobacco sample 0.20 g in 40 mL water for three hours. Finally, the brown mixture was filtered and the separated solution was poured to 50 mL and stored at 4 °C for later use in experiments after diluted to the mark.

RESULT AND DISCUSSION

Surface Characterization

The surface of the bare, activated, and *p*-ABSA grafted SPCE was examined using Fourier transform infrared (FT-IR), and Field emission scanning electron microscope (FESEM). The FT-IR results of the three electrodes bare, activated and *p*-ABSA grafted SPCE is depicted in (Figure 2). The broad OH stretching between 3000 cm^{-1} and 3500 cm^{-1} was observed in the activated

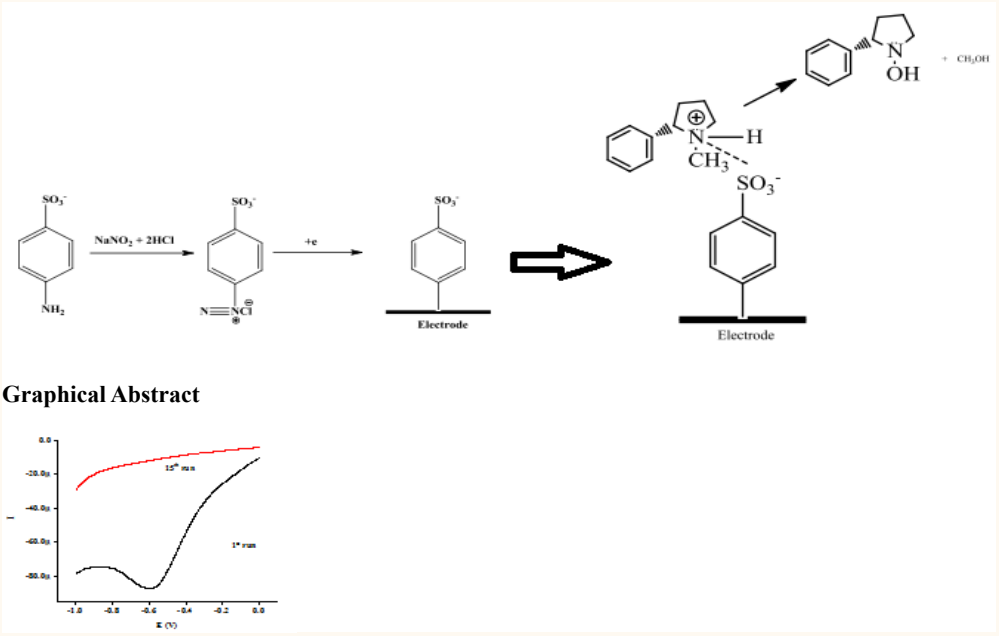

Figure 1 LSV for the diazotation mixture (10 mM $NaNO_2$ + 5 mM p-PABSA in 0.5 M HCl) in activated SPCE with the potential range of 0.0 to -1.0 at a scan rate of 100 mV s^{-1}.

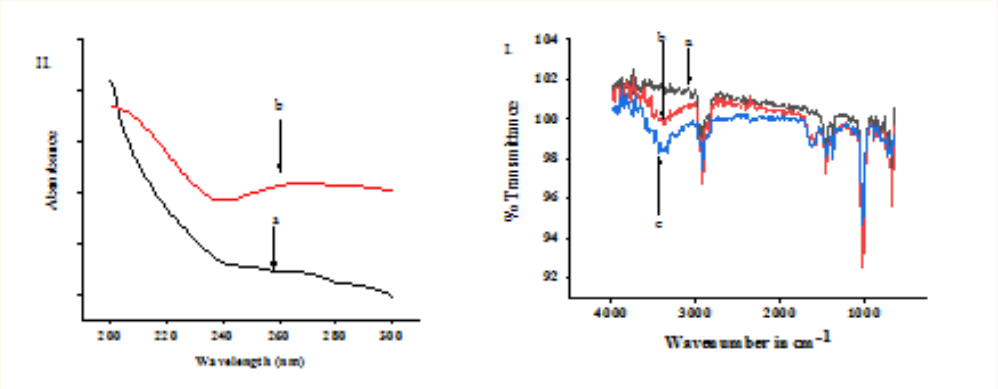

Figure 2 (I) FTIR spectrums of bare (a), activated (b), and p-ABSA grafted SPCE (c), (II) UV spectrum of bare SPCE (a) and p-ABSA grafted SPCE (b).

SPCE, and *p*-ABSA grafted SPCE [22]. The OH stretching in the *p*-ABSA grafted SPCE is broader than that of the activated one as a consequence of OH group presence in *p*-ABSA additional to its incorporation during activation. The sulfonic acid stretching peak observed in the 1373 cm^{-1} and the aromatic peak at 1635 cm^{-1} is a conformation for the grafting of *p*-ABSA on the surface of the electrode. The covalent attachment of *p*-ABSA was also confirmed by UV-Vis spectroscopic analysis, (Figure 3) shows a spectral band at 250 nm due to the presence of a benzene ring.

The bare SPCE resolved image depicted in [(Figure 4 (A)] indicates that the carbon surface is covered with a high content of graphite particles, and the image of activated SPCE in[Figure 4 (B)] reveals the surface morphological changes on bare SPCE caused during the activation. The bare SPCE surface is smooth and flat, but the electrochemical activation leads to the deterioration of the carbon surface. Roughness and porosity on the SPCE surface were observed after the activation. This rough and porous surface was probably due to the dissolution of the carbon by the basic media and exposing the oxidized carbon surface. And the high-resolution SEM shows that the *p*-ABSA grafted SPCE is highly dispersed and can be identified easily [Figure 4 (C)] .

Electrochemical characterization of p-ABSA modified electrode

Cyclic voltammetry using ferri/ferrocyanide couple was used as a tool to monitor the behavior of the modified electrodes. This tool was used to investigate the electron transfer or blocking behavior and use as a tool to confirm modifications of the electrode surface. The depicted result in (Figure 4) displays the characteristic ferri/ferrocyanide redox peak in the bare and activated SPCE but for *p*-ABSA grafted SPCE the redox peak shape was declined, and the potential peak separation is very high. This observation illustrates an effective covalent bond formation of *p*-ABSA with the electrode surface. The reason for the change is the negatively charged terminal sulfonic acid group that hinders the diffusion of the probe towards the electrode surface.

Electrochemical behavior of NIC at p-ABSA grafted SPCE

In order to determine the electrochemical behavior of the bare, activated, and *p*-ABSA grafted SPCE, towards 100 µM nicotine CV and SWV was performed in BRB solution (pH = 8). The resulted voltammograms in (Figure 5) reveal the irreversible oxidation peaks for nicotine. At the bare SPCE, no clear oxidation peak was observed, but in the activated one a small peak current was observed; moreover, higher current is observed at *p*-ABSA grafted SPCE at a positive potential + 0.896 V. The result indicates the *p*-ABSA grafted SPCE has high electrocatalytic activity towards nicotine compared with the activated SPCE.

The Effect of Scan Rate

To evaluate the electrochemical process at *p*-ABSA grafted SPCE whether it is diffusion or adsorption control, scan rate studies were taken place. The scan rate influence on the peak

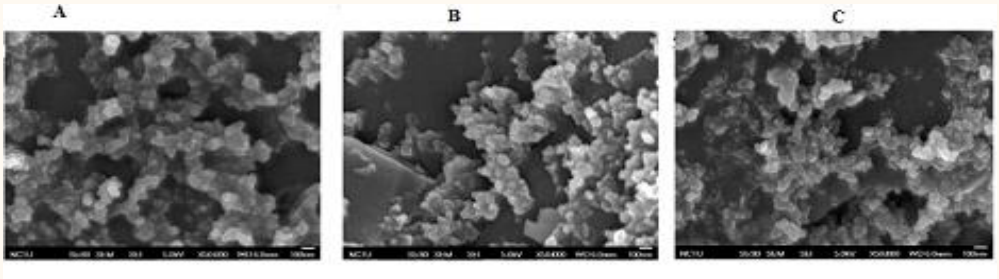

Figure 3 SEM images of bare SPCE (A) activated-SPCE (B) and p-ABSA grafted SPPCE (C).

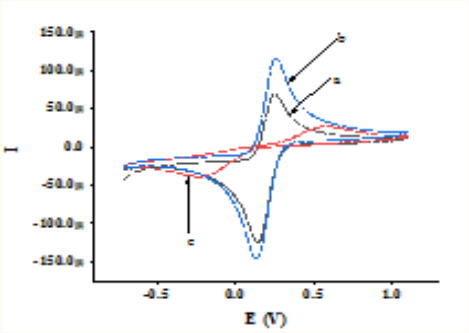

Figure 4 CV plots of 5 mM $[Fe(CN)_6]^{4-/3-}$ at; (a) bare SPCE, (b) activated SPCE and (c)*p*-ABSA/SPCE.

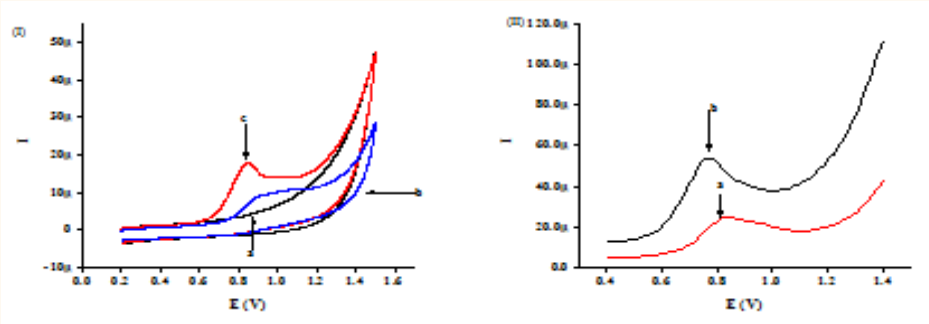

Figure 5 (I) CV of NIC in BRB solution pH 8 recorded in 0 µM NIC (a) 100 µM NIC in activated SPCE (b) *p*-ABSA grafted SPCE (c), (II) SWV of NIC in BRB solution pH 8 recorded 100 µM NIC in activated SPCE (a) and *p*-ABSA grafted SPCE (b).

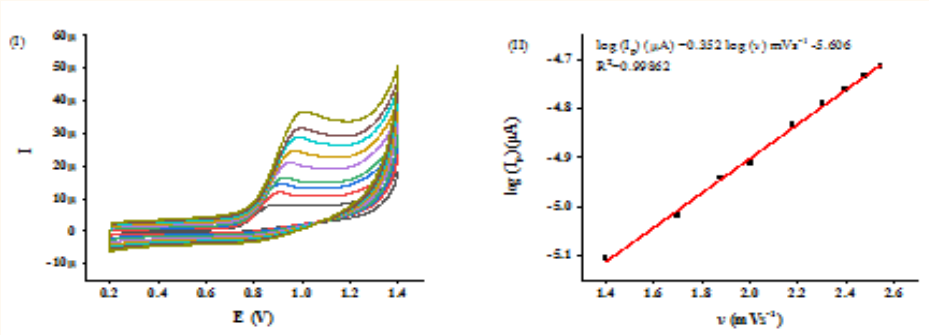

Figure 6 (I) CVs of 100 µM NIC at *p*-ABSA grafted SPCE in BRB solution (pH 8.0) at a different scan rates (0.025-0.300 V s^{-1}) (II) plot of logarithm peak current versus logarithm of scan rate in the range of 0.025-0.300 V s^{-1}.

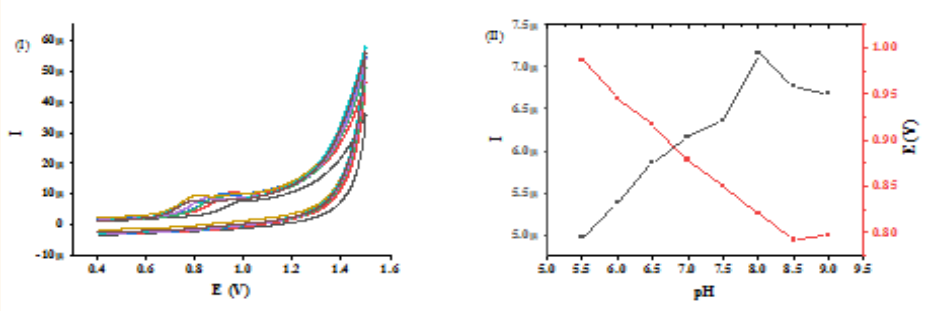

Figure 7 (I) CVs of 100 µM NIC in BRB solution by varying pH values with the range of 5.5–9.0 (II) Effect of the pH value on the peak current and peak potential of the NIC solution.

potentials and peak currents were investigated by CV on 100 µM CAP in BRB solution (pH 8.0) with varying the scan rates from 50 to 200 mV s^{-1}. An oxidation peak during the anodic scan from 0.2 to 1.4 V in all scan rates with positive shifts on peak potential was observed and this confirmed the oxidation is an irreversible. The plot of the logarithm of peak current versus the logarithm of scan rate gave a straight line with a slope of 0.352 with correlation coefficient 0.995, close to the theoretical value of 0.5 [23], so the electrode had a diffusion-controlled process.

The Effect of pH

The impact of pH in the determination of nicotine on *p*-ABSA grafted SPCE was evaluated by varying the pH in the ranges 5.5 to 9.0 and positive peak potentials shift with increasing pH were observed. Similarly, the peak current is increased when the pH was increased from 5.5 to 9.0 and decreased above the pH = 8.0. Nicotine which is a diacidic weak base has two pKa values, 8.02 and 3.12 which are due to the monoprotonated and diprotonated form respectively. At pH ≥ 9.0, nicotine, which is in un-protonated and alkaline form overweighs in the supporting electrolytes. The protonation of the pyrrolidine moiety of the nicotine at pH 7.0-8.0 forms the monoprotonated form and diprotonated form predominated at pH 2.0-2.7 [24&25]. The plot of peak potential with that of pH gave a linear relationship with regression equation: E (V) = -0.0638pH + 1.332 (R^2 = 0.9965). The value for the slope close to 0.0638 points out that the electron and proton number participating in the electrode are equal [26].

Optimization of SWV Parameters

For a higher signal and more sensitive determination of NIC at the modified electrode, the SWV technique was employed. A resolved oxidation peak was obtained for 100 µM NIC in BRB with pH 8.0. The SW parameters frequency, amplitude, and step potential effects on the current response were investigated by varying their values. Results obtained showed an increase in peak current with increasing the parameters. But the optimum values for step potential, amplitude, and frequency of 40 Hz were 10 mV, 60 mV, and 40 Hz respectively and are selected by considering the anodic peak shape and the magnitude of peak current.

The Effect of Accumulation Potential and Time

The effect of accumulation potential on the response for 100 µM nicotine was investigated between −0.5 and +0.5 V. Varying the accumulation potential with 15 s accumulation time, the peak current increased with rise in the potential starting from −0.5 V, and attain maximum value at 0.1 V. At potentials higher than 0.1 V, a decrease of current was observed. Therefore, 0.1 V was chosen as the optimum accumulation potential. Similarly, the accumulation time effect was studied between 15 and 75 s with an accumulation potential of 0.1 V and the maximum value was obtained at 45 s.

Determination of NIC by Square Wave Voltammetric Techniques

Employing the optimized measurable factors, the NIC determination was carried out using square wave voltammetric techniques. Figure 8 shows the SW voltammograms for varying the concentrations of NIC in BRB solution (pH 8.0) using *p*-ABSA grafted SPCE. Linear relation was achieved within the range of 0.5 to 300 µM for the plot of peak current as a function of concentration. The linear relationship resulted in the regression equation: Ip (µA) = 1.778 (µM) + 5.296 and R^2 = 0.99824 and the calculated limit of detection was 0.35 µM [27].

Offers the analytical efficiency of various modified electrodes and electrochemical strategies that have been formerly reported in the literature for the detection of NIC. The overall performance of the present sensor is superior to most of the preceding sensors reported in the literature in terms of sensitivity and linear dynamic range (Table 1), it is granted to the sulfonic acid functionalities grafted on the SPCE.

Carbon paste electrodes titanium oxide/poly(3,4-ethylenedioxythiophene)/Indium/tin oxide electrode, Pencil graphite electrode, Boron-doped diamond electrode, Boron-doped diamond electrode, poly(4-amino-3-hydro-xynaphthalene sulfonic acid) modified glassy carbon electrodes, Electrochemically activated glassy carbon electrodes, Multi-walled carbon nanotube modified glassy carbon electrode, Reduced graphene oxide/(E)-1-(4-((4-(phenylamino)phenyl)diazenyl) phenyl) ethanon modified Pencil graphite electrode, screen printed carbon electrode.

Interference Study

Possible interference in the detection of nicotine using *p*-ABSA grafted SPCE was investigated by adding the interferents to BRB solution pH 8 containing 100 µM of nicotine. All the analyzed interferents: Fe^{3+}, Mg^{2+}, Ca^{2+}, K^+, Na^+, NH_4^+, uric acid, and

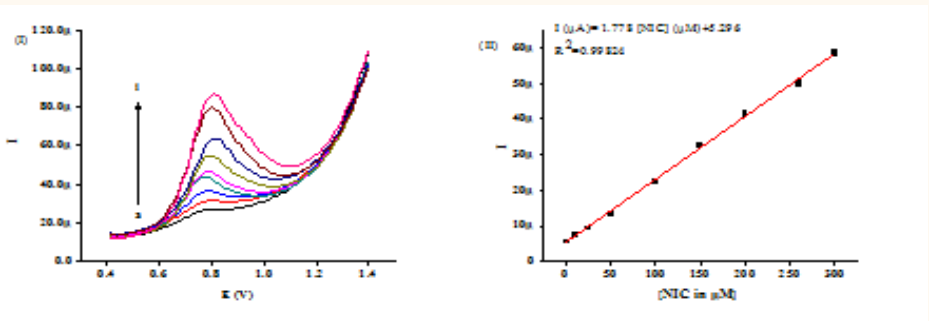

Figure 8 (I) SWVs for varying concentrations of NIC: 0.5, 10, 25, 50, 100, 150, 200, 260 and 300 µM in BRB solution pH 8.0 at p-ABSA grafted SPCE (II) The plot of peak current vs. NIC concentrations.

Table 1: Comparison of the performance of the proposed method with other electrochemical sensors used for the determination of NIC

Electrodes	Method	Linear Range (µM)	LOD (µM)	Reference
[a]CPE	SWV	50–500, 50–1000	6.1, 3.2	[25]
[b]TiO_2 /PEDOT/ITOE	AMP	0–5000	4.9	[28]
[c]PGE	SWV	7.6–107.5	2	[29]
[d]BDDE	SWV	5–500	3.1	[30]
[e]BDDE	DPV	0.5–202.5	0.3	[31]
[f]p-AHNSA/GCE	SWV	1–200	0.9	[26]
[g]EA/GCE	SWV	1–200	0.7	[32]
[h]MWCNT/GCE	DPV	31-1900	9.3	[33]
[i]RGO/DPA/PGE	DPV	31-1900	7.6	[34]
[j]SPCE	DPV	1-375	0.6	[35]
p-ABSA grafted SPCE	SWV	0.5-300	0.35	This Work

Table 2: Determination of nicotine levels urine samples using *p*-ABSA grafted SPCE (n=3).

Sample	Added (µM)	Found (µM)	Recovery (%)
Urine	15	15.88	105.9
	35	33.83	95.7
	65	67.94	104.5

Table 3: Determination of nicotine levels in Cigarette sample using *p*-ABSA grafted SPCE (n=3).

Sample	Added (µM)	Found (µM)	Recovery (%)
Cigarette	60	58.8	98.0
	160	165	103.0

glucose had no noticeable effect on the current responses of the nicotine with fifty-fold concentrations. For this reason, it can be inferred that these species do not significantly interfere in the determination of nicotine, and the modified electrode will be able to be applied for nicotine detection in the occurrence of the potential interfering species. Though the interfering substances commonly exist in human urine and cigarette samples, the determination of nicotine is not affected by their presence.

The practical applicability of *p*-ABSA grafted SPCE was assessed by analyzing cigarette samples and volunteer human urine samples. The samples for cigarette and urine were developed by diluting them with BRB solution pH 8. Recoveries of the samples were conducted by adding the standard volume of nicotine solution to the real samples. The obtained recovery results of cigarette and urine samples are portrayed in (Table 3) and (Table 4). The recovery data of the present study clearly shows that accurate detectio n of nicotine in cigarette and urine samples was achieved.

CONCLUSION

In conclusion, the successful grafting of *p*-ABSA on the surface of SPCE employing electrochemical methods was achieved. The FTIR and VU-VIS spectrum confirms the presence of aromatic and sulfonic acid functional groups and this is due to the grafting of *p*-ABSA on the SPCE surface. Although the conductivity of the *p*-ABSA grafted SPCE is lower than that of the bare SPCE, the electrocatalytic performance of it on nicotine is superior. Under optimum conditions, the *p*-ABSA grafted SPCE could detect nicotine over a linear range from 0.5 to 300 µ M with a low detection limit 0.35 µ M. In addition, the prepared electrode has been successfully employed for identifying nicotine content in cigarette product and urine samples within the range.

REFERENCES

1. Rahim S, Rauf A, Rauf, S, Shah M R, and Malik M I. Enhanced electrochemical response of a modified glassy carbon electrode by poly(2-vinlypyridine-bmethyl methacrylate) conjugated gold nanoparticles for detection of nicotine?.RSC Advances. 2018; 8: 35776–35786.

2. Hsia S L, Mischel A K, and Brody A L. Absolute Addiction Psychiatry Review. 2020. 105–120.

3. Benowitz N. Benowitz N. Clinical pharmacology of nicotine Clinical Pharmacology & Therapeutics.2008. 83: 531–541.

4. Karthika A, Karuppasamy P, Selvarajan S, Suganthi A, and Rajarajan M. Ultrasonics Sonochemistry, 2019; 55: 196–206.

5. Tizabi Y, Getachew B, Copeland R L and Aschner M. The FEBS Journal in 2021: a sharp reminder that science really matters. 2020; 287: 3656–3663.

6. Levent A, Yardim Y and Senturk Z. Electrochimica Acta, 2009; 55: 1–134.

7. Palazzolo D, Nelson J M, and Hudson Z. International Journal of Environmental Research and Public Health, 2019; 16: 3015.

8. Bansal M, Sharma M, Bullen C, and Svirskis D. International Journal of Environmental Research and Public Health. 2018; 15: 1737.

9. Pereira G R, Marchetti J M, and Bentley M V L B. A SIMPLE AND RAPID METHOD FOR NICOTINE ASSAY BY HPLC FROM CUTANEOUS MICRODIALYSIS SAMPLES. Analytical Letters. 2001; 34: 1669–1676.

10. Hossain A M, and Salehuddin S M. Analytical determination of nicotine in tobacco leaves by gas chromatography–mass spectrometry. Arab. J. Chem.2013.6: 275–278.

11. Pagano T, Difrancesco A G, Smith S B, George J, Wink G, et al. Determination of Nicotine Content and Delivery in Disposable Electronic Cigarettes Available in the United States by Gas Chromatography-Mass Spectrometry. Nicotine. 2015; 18: 700–707.

12. Lu G H and Ralapati S. Application of high-performance capillary electrophoresis to the quantitative analysis of nicotine and profiling of other alkaloids in ATF-regulated tobacco products. Electrophoresis. 1998; 19: 19–26.

13. Yang S S and Smetena I. Chromatographia. 1995; 40: 375–378.

14. Sun J, Du H and You T. Electrophoresis. 2011; 32: 2148–2154.

15. Willits C O, Swain M L, Connelly, J A, and Brice B A. Analytical Chemistry, 1950; 22: 430–433.

16. Acar E T and Atun G. Electroanalysis, 2018; 30: 2994–3002.

17. Zanoni B V. M, Rosa V L I, Pesquero, R C and Stradiotto R. N J. Braz. Chem. Soc. 1997; 8: 223-227.

18. Ramírez-Chan, D E, Fragoso-Soriano R. and González F J. Effect of Electrolyte Ions on the Formation, Electroactivity, and Rectification Properties of Films Obtained by Electrografting. Chem Electro Chem. 2019; 7: 904–913.

19. Nassef H M, Civit, L, Fragoso A and O'sullivan C. K. Amperometric sensing of ascorbic acid using a disposable screen-printed electrode modified with electrografted o-aminophenol film. Analyst. 2008; 133: 1736-1741.

20. Fletcher S. Advances in Electrochemical Sciences and Engineering Electrochemistry of Carbon Electrodes. 2015; 425–444.

21. Erdoğdu G, Yağci Ş Z and Savan E K. Turkish Journal of Pharmaceutical Sciences, 2019; 16: 450–456.

22. Compton G.R and Tanner E E L. How can Electrode Surface Modification Benefit Electroanalysis. Electroanalysis. 2018; 30: 1336–1341.

23. Wanga J, Pedreroa M, Sakslund H, Hammerichb O and Pingarronc, J. Analyst, 1990; 121: 345-350.

24. Stočes M , Švancara I. Electrochemical Behavior of Nicotine at Unmodified Carbon Paste Electrode and Its Determination in a Set of Refilling Liquids for Electronic Cigarettes. Electroanalysis. 2014; 26: 2655–2663.

25. Levent A, Yardim, Y and Senturk Z. Electrochim. Acta. 2009; 55: 190–195.

26. Xiong H, Zhao Y, Liu P, Zhang X and Wang S. Microchim. Acta, 2010; 16831–16836.

27. Sun T, Pan H, Mei Y, Zhang P, Zeng D, Liu X, Rong S and Chang D. Journal of Applied Electrochemistry , 2018, 49, 261–270.

28. Suffredini B H, Santos C M, Souza D, Codognoto L, et al. Machado, S.A.S. , and Avaca, L.A. Anal. Lett., 2005; 38: 116587–1599.

29. Švorc Ľ, Stanković, D.M and Kalcher K. Single crystal diamond wafers for high power electronics. Diam. Relat. Mater. 2014; 42: 168–175.

30. Geto A, Amare M, Tessema M and Admassie S. Voltammetric Determination of Nicotine at Poly(4-Amino-3-Hydroxynaphthalene Sulfonic Acid)-Modified Glassy Carbon Electrode. Electroanalysis. 2012; 24: 659–665.

31. Kassa H, Geto, A and Admassie S. Bull. Chem. Soc. Eth. 2013; 27.

32. Jing Y, Yu B , Li P, Xiong B, Cheng Y, et al. Synthesis of graphene/DPA composite for determination of nicotine in tobacco products. Sci. Rep. 2017; 7: 14332.

33. Lo B, W T, Aldous L and Compton G R. Sens. Actuators, B. 2012; 162: 361–368.

34. Jing Y, Yu B , Li P , Xiong B , Cheng Y, et at. Synthesis of graphene/DPA composite for determination of nicotine in tobacco products. Sci. Rep. 2017; 7: 14332.

35. Goodarzi , Maghrebi, M, Zavareh A F, Mokhtari-Hosseini Z.-B, Ebrahimi-Hoseinzadeh, et al. Journal of Nanostructure in Chemistry. 2015; 5: 237–242.

Cite this article

Hailu T, Li YK, Tessema M (2021) Electrochemical Determination of Nicotine in Cigarette, and Urine Using para-Aminobenzene Sulfonic Acid Grafted Screen Printed Carbon Electrode. JSM Chem 8(1): 1055.